Lab-scale demonstration of thermochemical energy storage with NH_3 and impregnated-loaded zeolites

Danny Müller,[1*] Christian Knoll,[1,2] Georg Gravogl,[1,3] Andreas Werner,[4] Michael Harasek,[2] Ronald Miletich,[3] Peter Weinberger[1]

[1] Institute of Applied Synthetic Chemistry, TU Wien, Getreidemarkt 9/163-AC, 1060 Vienna, Austria

[2] Institute of Chemical, Environmental & Biological Engineering, TU Wien, Getreidemarkt 9, 1060 Vienna, Austria

[3] Institut für Mineralogie und Kristallographie, University of Vienna, Althanstraße 14, 1090 Vienna, Austria

[4] Institute for Energy Systems and Thermodynamics, TU Wien, Getreidemarkt 9/302, 1060 Vienna, Austria

danny.mueller@tuwien.ac.at

Abstract

High energy densities are one key-feature of thermochemical energy storage materials. Among the substance classes featuring the highest energy densities are oxides and carbonates, having both operational temperature profiles between 800 °C - 1200 °C. Comparable high energy contents are provided by the reaction between ammonia and (transition) metal salts, operable in a medium-temperature range between 150 °C - 450 °C. Due to the toxicity of ammonia a closed cycle preventing the release of ammonia to the surrounding environment would be necessary.

Herein, $CuSO_4$ and $CuCl_2$ are investigated in a laboratory scale reactor for their application in thermochemical energy storage with ammonia as reactive gas. In the current setup after 80 seconds peak temperatures of 312 °C and 238 °C respectively were measured. To circumvent the notable volume expansion during the reaction with ammonia, both copper salts were loaded on zeolite 13X, yielding matrix-supported composite materials. Operation of those materials in the laboratory scale reactor under ammonia revealed, that the rapid temperature increase and the high peak temperatures could be retained, simultaneously simplifying the handling of the materials.

Keywords: copper salts, copper ammoniates, laboratory scale reactor, thermochemical energy storage

1. Introduction

Increased awareness of a necessary reduction of greenhouse gasses in relation to energy production stimulated an ongoing reorientation of the energy market. (IEA, 2014, Paris agreement, 2015) Environmentally benign energy production with increasing percentages of renewable energy, a sustainable energy management and a responsible use of the produced energy led to a multiplicity of innovative approaches, complying the climate targets. (Keith Shine, 2005) Related to this development are also the increase of energy efficiency, especially in context of electricity production, as according to the IEA about 2/3 of the therefore used energy are lost in form of waste heat. (IEA, 2011)

Optimizing the waste heat management encouraged research to develop recycling methods for so far lost waste heat. (Bauer et al., 2012; Hasnain, 1998) One auspicious approach due to its broad application profile is the thermal storage of waste heat by sensible, (Zhang et al., 2016) latent (Zalba et al., 2003) or thermochemical energy storage materials. (Abedin; A.H. 2011; Cot-Gores et al.; 2012, T. Yan, 2015) Thermochemical energy storage (TCES) takes a very prominent position amongst these approaches, as highest storage densities, loss-less storage, a broad

doi:10.18086/swc.2017.14.04 Available at http://proceedings.ises.org

operational temperature profile and fast reaction times allow for a flexible application in domestic and industrial environments, compatible with waste heat temperatures between 30 °C and above 1200 °C.(T. Yan, 2015)

Depending on the available waste heat source, the suitable materials may be selected from an ample catalogue of principally suitable reactions, ranked according to their storage density and application temperature.(Deutsch et al., 2016) On the lower end of the temperature spectrum are located salt hydrates for *e.g.* application in energy efficient housing projects,(van Essen et al., 2009) whereas the high temperature end around 800 °C - 1200 °C is covered by carbonates and oxides, complementing *e.g.* concentrating solar power plants (CSP) during non-operational times. (Pardo et al., 2014) For the medium temperature region between 150 °C - 450 °C so far mainly hydroxide / oxide reactions (Criado et al., 2014) or metal hydrides were considered. (T. Yan, 2015)

A so far widely neglected class of TCES-materials operating in this temperature range are (transition) metal salt ammoniates, featuring notably high storage densities, comparable to redox-active metal oxides. Although, first reports on reactions of NH_3 with salts for energy storage purposes date back to the 80's, (Dunlap, 1982) until today only a handful of publications dealing with the reaction between $CoCl_2$, (AidounTernan, 2001; Trudel et al., 1999) $MnCl_2$ (Jiang et al., 2016) or $ZnCl_2$ and NH_3 (Dunlap, 1982) is known. Concepts for NH_3 in energy storage technology relate mainly on the NH_3 formation / splitting in combination with solar power. (Dunn et al., 2012; Lavine et al., 2016; Lepinasse-Spinner, 1994; Lovegrove et al., 1999; 2004)

One major obstacle of NH_3 is its inherent toxicity. Therefore, to enable thermochemical energy storage based on NH_3-metal salt reactions, a closed reactor design, avoiding any release of NH_3, would be necessary. For this purpose, in the present work a feasibility study of a NH_3-based storage reaction, using $CuSO_4$ / $CuCl_2$ loaded on zeolite 13X in a hermetically closed laboratory scale reactor, is presented.

2. Experimental

2.1 Material

$CuSO_4$ was obtained by drying $CuSO_4 \cdot 5H_2O$ for 3 h at 400 °C in an electric furnace. All other materials were commercially obtained and used as supplied.

The copper-loaded zeolites **13X-SO_4** and **13X-Cl** were prepared by soaking zeolite 13X for 30 minutes in a saturated solution of $CuSO_4 \cdot 5H_2O$ or $CuCl_2 \cdot 2H_2O$. The zeolite was rinsed with water and dried for 2 h at 150 °C under vacuum, before the soaking procedure was repeated. After rinsing with water, the loaded zeolite was dried for 2 h at 400 °C and stored after cooling in a desiccator. The Cu-loading was determined gravimetrically and by X-Ray fluorescence spectroscopy with 0.16 g $CuSO_4$, and 0.09 g $CuCl_2$ per gram of zeolite.

For preparation of the partially reduced copper-loaded zeolites, dried samples of **13X-SO_4** and **13X-Cl** were soaked for 15 minutes in a 10 % aqueous solution of $N_2H_4 \cdot H_2O$. Due to the exothermic reaction no additional heating was necessary to keep the reaction constantly at 65 °C.

2.2 Thermal Analysis

For thermal analysis a Netzsch TGA/DSC 449 C Jupiter ® equipped with a water vapour furnace including an air-cooled double jacket was used. The oven operates between 25 °C and 1250 °C, regulated by an S-type thermocouple. NH_3 gas was 99.98 % and obtained from Messer. The gas flow was set to 100 ml min^{-1}, controlled and mixed with Vögtlin Instruments "red-y" mass flow controllers. A sample mass of 10 mg in an open aluminum crucible was used for all experiments with heating and cooling rates of 10 °C min^{-1}. The DSC was calibrated according to the procedure suggested by Netzsch, using the In, Sn, Bi, Zn, Al and Ag standards provided by the manufacturer.

2.3 Reactor-setup

For the experiments in a closed system a reactor consisting of two separated chambers connected via a tap was used. Both chambers had an inner diameter of 40 mm and a length of 200 mm. The reaction chamber was fitted with a manometer to monitor the internal pressure, as well with two K-type thermocouples positioned in the middle of the chamber (T1 and T2) and a further K-type thermocouple on the outside (T3). The reaction chamber

was loaded with the dried copper salt / copper-loaded zeolite and the whole system was evacuated for 10 minutes. The tap between reaction chamber and NH_3-chamber was closed, and NH_3 liquified in the NH_3-chamber being cooled down to – 50 °C. After 10 minutes the tap to the NH_3 cylinder was closed and the NH_3-chamber warmed to room-temperature. Once the reactor had established a thermal equilibrium with the surrounding, the tap between NH_3-chamber and reaction chamber was opened to start the reaction (discharging of the storage material). Due to the excess of NH_3 during all experiments a pressure of 6 bar was obtained in the system.

For all experiments 250 ml of material were charged to the reactor.

2.4 Scanning Electron Microscopy

SEM images were recorded on gold coated samples with a Quanta 200 SEM instrument from FEI under low-vacuum at a water vapor pressure of 80 Pa to prevent electrostatic charging.

3. Results and Discussion

3.1 Reaction between NH_3 and $CuSO_4$ / $CuCl_2$

The reaction between NH_3 and $CuSO_4$ / $CuCl_2$ – although, mainly in aqueous solutions – is a well-known, colorful reaction for demonstration of simple coordination chemistry in undergraduate-laboratories. Even in the case of mixing the aqueous solutions of NH_3 and $CuSO_4$ an increase of the reaction temperature is observed.

For the gas-solid reaction between NH_3 and $CuSO_4$ / $CuCl_2$ energy-densities of 1.77 MJ kg^{-1} and 2.20 MJ kg^{-1} were obtained by differential scanning calorimetry. These values are highly comparable to the benchmark of metal-oxide redox-reactions, featuring the highest energy densities among the various TCES-materials. Even more important for a potential TCES-material, thermogravimetry evidenced a full reversibility of the NH_3- coordination, thus by heating the formed ammine-complexes to 350 °C the initial copper salts are restored (see figure S1). Based on the decomposition of the copper-ammine complexes their composition was determined as $[Cu(NH_3)_4]SO_4$ and $[Cu(NH_3)_6]Cl_2$, thus $CuSO_4$ reacting with 4 equivalents of NH_3, $CuCl_2$ with 6.

The experimental setup selected for the gas-solid reaction between NH_3 and the anhydrous copper salts on a laboratory scale is shown in figure 1.

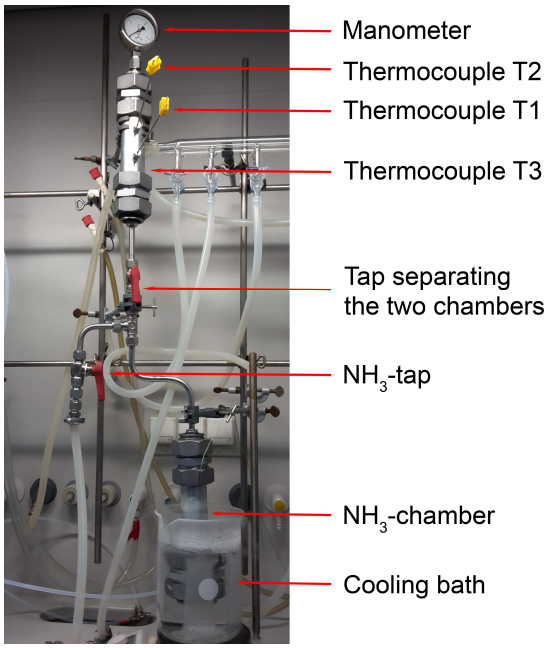

Fig. 1: Laboratory scale reactor for the gas-solid reaction between NH_3 and copper salts in a closed system

Based on the necessity of a closed system preventing the release of NH_3, a reactor with two chambers, separated

by a tap, was selected. The copper salt is situated in the reaction chamber (upper part). After evacuation of the complete system the tap between the two chambers is closed and NH_3 is condensed into the precooled NH_3-chamber. Once the NH_3-tap is closed, the NH_3-chamber is warmed to room-temperature and the reaction is started by opening the tap between the two chambers. The temperature gradient during the reaction was monitored by the 3 thermocouples T1-T3, T1 and T2 placed inside, in the middle of the reactor, T3 on the outside to follow the heat conductance. Due to the NH_3-excess used, through all experiments a constant pressure around 6 bar was obtained.

In figure 2 the temperature plots for the formation of $[Cu(NH_3)_4]SO_4$ (figure 2a) and $[Cu(NH_3)_6]Cl_2$ (figure 2b) are given.

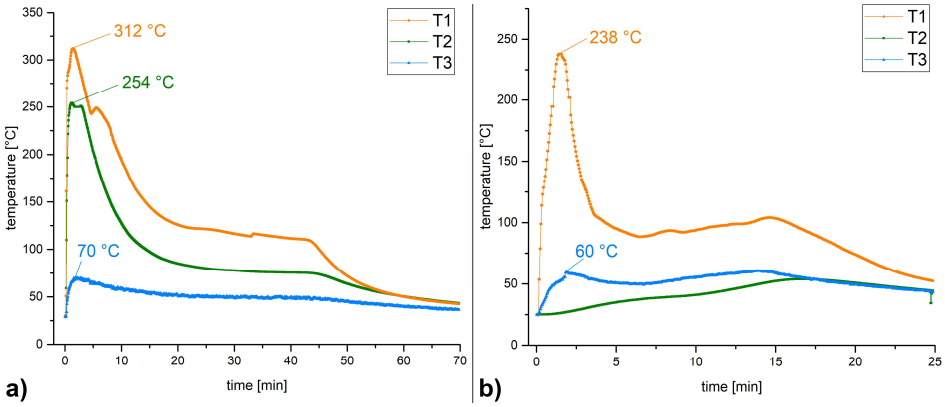

Fig. 2: Temperature plots for the formation of a) $[Cu(NH_3)_4]SO_4$ and b) $[Cu(NH_3)_6]Cl_2$ in the reactor

For both experiments starting with the opening of the tap between the two chambers an extremely fast increase of the internal temperature is observed. For $CuSO_4$ the peak temperature of 312 °C* is reached after 80 seconds, after 10 seconds T1 exceeds already 160 °C. In the case of $CuCl_2$ a peak temperature of 238 °C was reached after 90 seconds.

Both experiments are highly encouraging, as such extremely fast reactions with concomitant high temperature differences are notably rare for thermochemical energy storage materials. Nevertheless, the packed bed using the pure metal salts in the reaction chamber cannot be considered ideal, as due to the extreme volume work during the reaction a compacting / sintering process of the material occurs, deteriorating permeability of the packed bed and thus hampering the completeness of the reaction. In the case of $CuSO_4$ after the reaction the former loose powder had turned into a solid brick, which had to be removed mechanically from the reaction chamber. Additionally, from the bottom to the top of the packed bed the completeness of reaction was notably affected: Whereas, in the bottom the dark blue $[Cu(NH_3)_4]SO_4$ was formed, on the top only a slight blue color of the former white material was observed. The kinks and sudden increases in the temperature profile are attributed to the volume work of the material, varying permeability of the continuously expanding packed bed.

In the case of $CuCl_2$, although with the observed peak temperature of 238 °C the melting point of $[Cu(NH_3)_6]Cl_2$ was not exceeded, due to partial overheating near to the bottom of the reaction chamber a dark black-bluish molten residue in the reactor was formed immediately. As the thermocouple T1 was above this molten mass, the observed peak temperature was lower than in the case of $CuSO_4$ (see figure S2). Additional, nearly 2/3 of the reactors' content did not react, as the NH_3 could not pass the molten salt / ammoniate mass. Therefore, also thermocouple T2 featured only very low temperatures and the temperature in the reactor had dropped within 25 minutes significantly.

The slow decrease of the temperature profile, retaining for some extended period temperatures above 100 °C, followed by a sudden decrease of the temperature is caused by the stepwise reaction of the copper salts with NH_3. As seen from the thermogravimetric decomposition in figure S1, for the consecutive addition or removal of each of the NH_3-ligands different equilibrium / decomposition temperatures are found. Therefore, with the initial temperature rise the reaction temperature is too high to allow for complete reaction. Coming to lower

* The difference between T1 and T2 is attributed to the linear progression of the reaction zone and sintering of the material, notably affecting permeability of the packed bed.

temperatures, the further coordination of NH_3 is enabled, still releasing notable heat and thus keeping the temperature almost constant unless the reactant is consumed.

In figure 3 a time-dependent series of infrared-images, visualizing the temperature increase and slow decrease during the reaction of NH_3 with $CuSO_4$ at the outside of the reactor is shown.

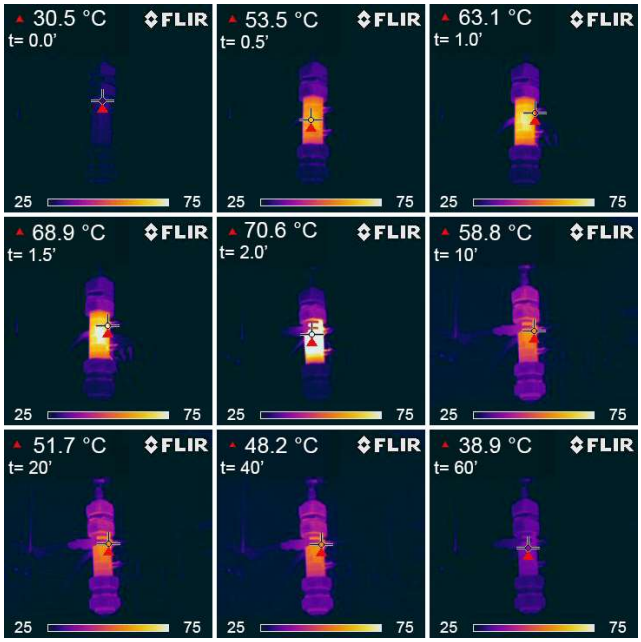

Fig. 3: Infrared-images of the reactor during the reaction of NH_3 with $CuSO_4$ at different time steps as indicated

Already after 30 seconds the temperature of the reactor walls had increased about 23 °C, reaching its maximum of 70.6 °C after 120 seconds. For the next 50 minutes a nearly constant temperature of 50 °C was observed. The temperature distribution in the IR-image after 40 minutes clearly shows, that the reaction was still ongoing.

The extreme volume work occurring on coordination of NH_3 to both copper salts becomes evident comparing the crystallographic parameters for the four different materials in table 1 (although, for $[Cu(NH_3)_4]SO_4$ only the monohydrate is found in the ICSD-database).

Tab. 1: Crystallographic parameters for $CuSO_4$, $CuCl_2$ and the corresponding NH_3-complexes

	$CuSO_4$	**$CuCl_2$**	**$[Cu(NH_3)_4]SO_4 \cdot H_2O$**	**$[Cu(NH_3)_6]Cl_2$**
	orthorhombic	monoclinic	orthorhombic	tetragonal
Space group	*P* n m a	*C* 1 2/m 1	*P* b n m	*F* 4/m m m
Nr°	62	12	62	139
Z	4	2	4	4
a [Å]	8.3976(1)	6.9038(9)	12.12	10.375(7)
b [Å]	6.70382(9)	3.2995(4)	10.66	10.375(7)
c [Å]	4.82443(8)	6.824(1)	7.07	9.481(11)
α [°]	90	90	90	90
β [°]	90	122.197(8)	90	90
γ [°]	90	90	90	90

V [Å^3]	271.6	131.54	913.44	1020.54

Based on the unit-cell volumes given in table 1, for $CuSO_4$ a 3.4-fold, for $CuCl_2$ a 3.9-fold volume expansion during the reaction with NH_3 is obtained.

To circumvent, or at least decrease the expansion of the material, causing considerable issues on larger (or applicational) scale, allow for a better permeability of the packed bed and control the temperature release during the reaction, the impregnation of zeolite 13X with $CuSO_4$ and $CuCl_2$ was chosen.

3.2 Reaction between NH_3 and matrix-supported $CuSO_4$ / $CuCl_2$

The $CuSO_4$ / $CuCl_2$ loaded zeolite samples (**13X-SO_4** and **13X-Cl**) were obtained as described in the experimental section, having a greenish-brown color after drying in the furnace (see figure S3). The copper-loading was determined gravimetrically and by X-Ray fluorescence spectroscopy with 0.16 g $CuSO_4$, and 0.09 g $CuCl_2$ per gram of zeolite.

Of course, the better handling and limited volume expansion goes to the expense of a much lower copper content compared to the pure salts, relating to a lower energy content and thus decreased reaction temperature. Due to the matrix-support also the heat transfer is affected. Therefore, externally copper-coated samples were prepared by reducing the external layer of copper-salts on the zeolite by hydrazine hydrate (see experimental), which should improve the thermal conductivity of the material.

To compare the performance of the various matrix-supported copper salts in the reactor, the same approach as described for the pure copper salts was chosen. In figure 3 the temperature plots of the experiments using **13X-SO_4** (figure 4a) and **13X-Cl** (figure 4b), and their partially reduced equivalents **13X-SO_4_Cu** (figure 4c) and **13X-Cl_Cu** (figure 4d) are shown.

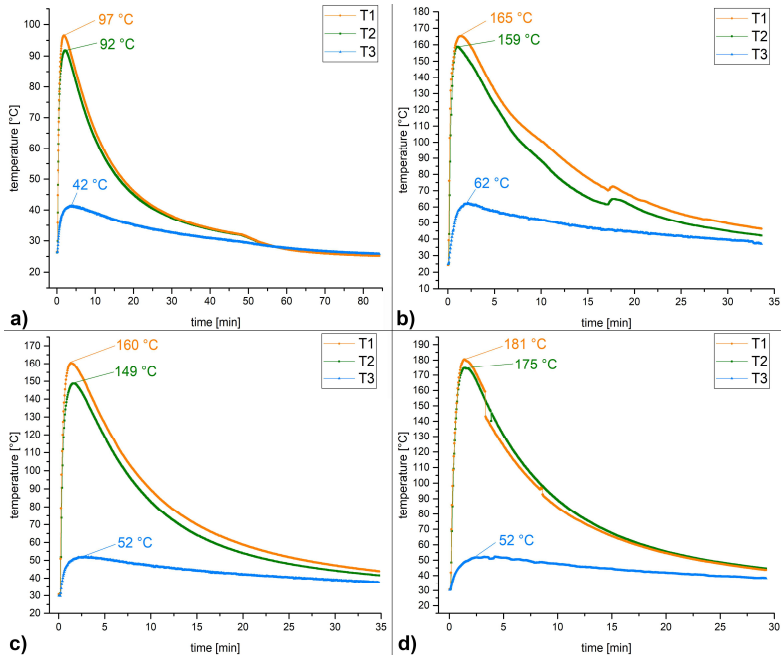

Fig. 4: Temperature plots for the reaction of NH_3 with a) 13X-SO_4 b) 13X-Cl c) 13X-SO_4_Cu d) 13X-Cl_Cu in the reactor

The prior observed temperature rise after opening the tap between the two chambers was also found in the present experiments, in all cases reaching the maximal temperature within 90 seconds. This finding is very promising, stating, that although the copper salts was heavily ‘diluted’ by loading on the matrix, its performance is still outstanding for a TCES-material. In these experiments also the temperature difference between T1 and T2 was reduced, as a notably better permeability of the packed bed was achieved. It should be emphasized, that due to the

particle shape of the zeolite the contact between thermocouple and material was less efficient as in the previous experiments. In this respect, the partial reduction of the copper salts on the zeolite matrix, yielding a better thermal conductivity was found quite efficient, as in the experiments with **13X-SO_4_Cu** (figure 4c) and **13X-Cl_Cu** (figure 4d) notably higher peak temperatures were observed. Especially, in the case of **13X-SO_4_Cu** (figure 4c) the impact of the external Cu-coating increased the measured temperature about 60 °C. The discontinuities in the temperature plots of **13X-Cl** and **13X-Cl_Cu** are attributed to slight movements of the packed bed, affecting the contact between thermocouple and zeolite particles.

A control experiment with a mixed packed bed loading of **13X-Cl** and 10 % copper turnings (figure S4) showed a decreased temperature output (figure S5) even compared to the experiment using unmodified **13X-Cl**. It seems, that in the case of the matrix-loaded copper salts even a further 10 % dilution has a negative impact on the highest achievable reaction temperature.

The use of matrix-supported copper salts in the reactor experiments turned out to be quite promising, as still the fast temperature increase and notably high peak temperature was retained, at the same time avoiding the volume expansion of the material during the reaction.

4. Conclusion

The reaction between NH_3 and $CuSO_4$ / $CuCl_2$ was investigated for their feasibility as thermochemical energy storage process. Initial requirement was the operation in a closed system to prevent release of NH_3 to the surrounding environment due to its toxicity. For this purpose, a two-chamber reactor setup with the reaction chamber and the NH_3-chamber – loaded by condensation of NH_3 at -50 °C – was chosen.

For the pure copper salts 80 seconds after beginning of the reaction the peak temperatures of 312 °C ($CuSO_4$) and 238 °C ($CuCl_2$) were obtained. Such an abrupt and remarkable temperature increase is quite outstanding and very promising for a high-end technological applicability of thermochemical storage materials. The reaction temperature is kept for about 40 minutes around 100 °C, as the stepwise coordination of NH_3-ligands to the copper salts continuously releases heat until the reaction is complete. The only and major drawback of such an operation is the extreme volume work during the reaction accounting up to a 3.9-fold volume expansion in the case of $CuCl_2$. This causes a sintering and condensing of the packed bed, affecting completeness of the reaction due to very limited permeability of the bed and complicates the handling, as the reacted material needs mechanical force to be removed from the reactor. In the case of $CuCl_2$ due to initial high reaction temperatures, exceeding locally the melting point of the $[Cu(NH_3)_6]Cl_2$ the reaction product is obtained as massive solid.

To allow for a better handling, but retain the promising reactivity, both $CuSO_4$ and $CuCl_2$ were loaded on zeolite 13X, resulting in matrix-supported copper salts. In this case the volume expansion during the reaction is nearly eliminated, concomitantly retaining high initial peak temperatures and fast energy release on reaction with NH_3. To ensure a better heat conductivity, partial reduction of the copper on the outside of the zeolite particles was accomplished by treatment of the composite materials with hydrazine hydrate. The thereby obtained externally copper coated, copper salt loaded materials revealed a much better thermal conductivity, leading to the observation of higher peak temperatures.

As the main objective of the present work was a feasibility study on the reaction of NH_3 with copper salts, respectively matrix-supported copper salts, the main subject of continuative studies will be the optimization of the heat output / heat transfer. Design and operation of the reactor / process will need some improvement to efficiently use and transfer the released heat.

5. References

1. IEA, 2014. Heating without global warming: Market developments and policy considerations for renewable heat.
2. Treatie, U.N., 2015. Paris agreement, No. 54113,
3. Keith Shine, J.F., Kinfe Hailemariam, Nicola Stuber, 2005. Alternatives to the Global Warming Potential for Comparing Climate Impacts of Emissions of Greenhouse Gases. climatic change 3, 281-302.
4. IEA, 2011. Co-generation and Renewables. Solutions for a low-carbon energy future. https://www.iea.org/publications/freepublications/publication/co-generation-and-renewables-solutions-for-a-low-carbon-energy-future.html
5. Bauer, T., et al., 2012. Thermal Energy Storage Materials and Systems. Annual Review of Heat Transfer 15, 131-177.
6. Hasnain, S.M., 1998. Review on sustainable thermal energy storage technologies, Part I: heat storage materials and techniques. Energy Conversion and Management 11, 1127-1138.
7. Zhang, H., et al., 2016. Thermal energy storage: Recent developments and practical aspects. Progress in Energy and Combustion Science 1-40.
8. Zalba, B., et al., 2003. Review on thermal energy storage with phase change: materials, heat transfer analysis and applications. Applied Thermal Engineering 3, 251-283.
9. Ali H. Abedin, M.A.R., 2011. A Critical Review of Thermochemical Energy Storage Systems. The Open Renewable Energy Journal 42-46.
10. Cot-Gores, J., A. Castell, and L.F. Cabeza, 2012. Thermochemical energy storage and conversion: A-state-of-the-art review of the experimental research under practical conditions. Renewable and Sustainable Energy Reviews 7, 5207-5224.
11. T. Yan, R.Z.W., T. X. Li, L.W.Wang, Ishugah T. Fred, 2015. A review of promising candidate reactions for chemical heat storage. Renewable and Sustainable Energy Reviews 13-31.
12. Deutsch, M., et al., 2016. Systematic search algorithm for potential thermochemical energy storage systems. Applied Energy 113-120.
13. van Essen, V.M., et al., 2009. Characterization of Salt Hydrates for Compact Seasonal Thermochemical Storage. 825-830.
14. Pardo, P., et al., 2014. A review on high temperature thermochemical heat energy storage. Renewable and Sustainable Energy Reviews 591-610.
15. Criado, Y.A., M. Alonso, and J.C. Abanades, 2014. Kinetics of the CaO/Ca(OH)2Hydration/Dehydration Reaction for Thermochemical Energy Storage Applications. Industrial & Engineering Chemistry Research 32, 12594-12601.
16. Dunlap, R.M., *Thermochemical energy storage and mechanical energy converter system*. 1982, Google Patents.
17. Aidoun, Z. and M. Ternan, 2001. Pseudo-stable transitions and instability in chemical heat pumps: the NH3–CoCl2 system. Applied Thermal Engineering 10, 1019-1034.
18. Trudel, J., S. Hosatte, and M. Ternan, 1999. Solid–gas equilibrium in chemical heat pumps: the NH_3–$CoCl_2$ system. Applied Thermal Engineering 5, 495-511.
19. Jiang, L., et al., 2016. Experimental investigation on a $MnCl_2$ –$CaCl_2$ –NH_3 thermal energy storage system. Renewable Energy 130-136.
20. Dunn, R., K. Lovegrove, and G. Burgess, 2012. A Review of Ammonia-Based Thermochemical Energy Storage for Concentrating Solar Power. Proceedings of the IEEE 2, 391-400.
21. Lavine, A.S., et al., 2016. Thermochemical energy storage with ammonia: Aiming for the sunshot cost target. 050028.
22. Lepinasse, E. and B. Spinner, 1994. Production de froid par couplage de réacteurs solide-gaz I: Analyse des performances de tels systèmes. International Journal of Refrigeration 5, 309-322.
23. Lovegrove, K., H. Kreetz, and A. Luzzi, 1999. The first ammonia based solar thermochemical energy storage demonstration. Le Journal de Physique IV PR3, Pr3-581-Pr3-586.
24. Lovegrove, K., et al., 2004. Developing ammonia based thermochemical energy storage for dish power plants. Solar Energy 1-3, 331-337.

6. Appendix

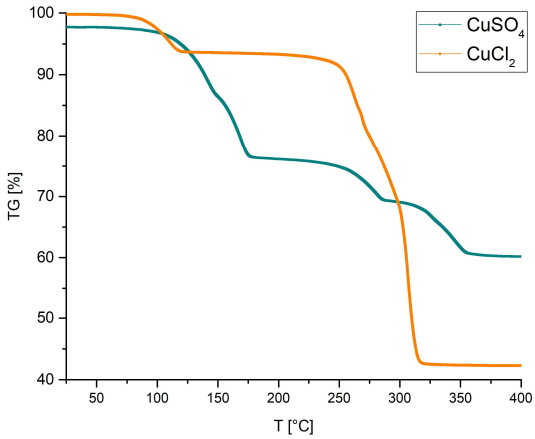

Fig. S1: Thermogravimetric decomposition of $[Cu(NH_3)_4]SO_4$ and $[Cu(NH_3)_5]Cl_2$

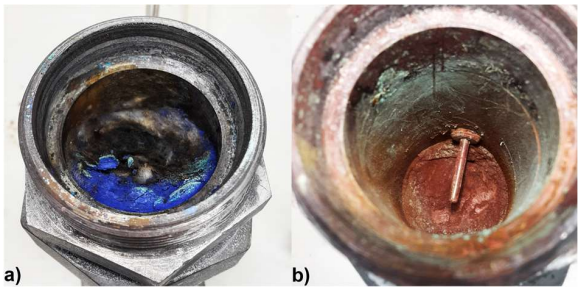

Fig. S2: Molten residue of $[Cu(NH_3)_6]Cl_2$ after the reaction a) molten residue on the bottom b) unreacted $CuCl_2$ on the top with thermocouple T2

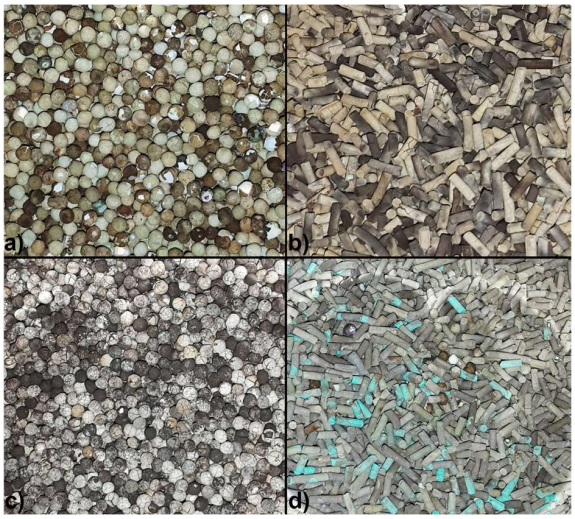

Fig. S3: Images of copper-impregnated zeolite 13X a) 13X-SO_4 b) 13X-Cl, c) 13-X-SO_4 after reaction with NH_3, c) 13-X-Cl_2 after reaction with NH_3

Fig. S4: A mixed packed bed loading of 13X-Cl and Cu-turnings

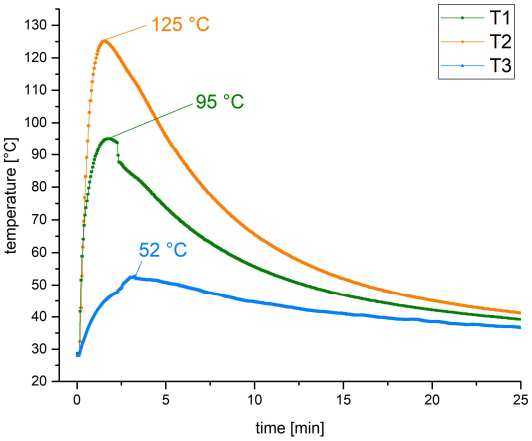

Fig. S5: Temperature plot for the reaction of NH_3 with a mixed packed bed loading of 13X-Cl and Cu-turnings